Chapter 5

Choice of precipitant in precursor for synthesis of CuMnOx catalysts

5. General

The redox reaction has been proposed to explain that the CuMnOx catalyst activity, i.e. an electron transfer between copper and manganese cations within the spinel lattice. The incidence of individual phases and their quantitative proportions depends not only on the precipitation conditions, such as temperature, pH and concentrations of the reactant solutions but also on the way of precipitate was aged [Gardner and Hoflund 1991; Liu *et al.,* 2016]. Ageing of the precipitate in the mother liquor is a common procedure that is use in the preparation process. The precipitate obtained by co-precipitation leads to the phase changes towards thermodynamically more stable structures [Kondrat *et al.,* 2011]. Activity of the catalyst for CO oxidation strongly depends on the combination of precipitant and precursor anions present in a catalyst. With the same precipitant, the catalysts prepared with acetate as a precursor resulted in a better catalytic activity than that of the prepared with nitrates as a precursor [Cai *et al.,* 2012]. The precipitant shows the greatest influence on the crystalline phases of the catalyst while the precursor shows a greater effect on the number of catalytic active sites which are directly related to the CO oxidation. The choice of precipitant in the precursor is important in designing the most efficient CO oxidation catalyst.

The success of CuMnOx catalyst has encouraged a great deal of fundamental work dedicated to instructive the role played by each component and the nature of active sites. The activity of CuMnOx catalyst depends upon the structure of the catalyst precursor and their preparation route [Cole *et al.,* 2010; Fuzhen *et al.,* 2015]. Recently, Tang *et al.* have synthesized the nano-crystalline CuMnOx catalysts using the

supercritical anti-solvent precipitation method and found them to be more than twice as active as the conventionally prepared Hopcalite catalysts for CO oxidation. They recognized the high catalytic activity of the nano-crystalline and homogeneous nature of the synthesized CuMnOx catalyst [Tang *et al.,* 2011]. The presence of manganese oxide is likely to facilitate the reduction of copper oxide, involving coordination between CuO and MnO_2, the manganese oxide acting as an oxygen donor and copper oxide acts as an oxygen acceptor. The precipitants used in the precursors to change the crystalline phase of the catalysts [He *et al.,* 2017].

The present work was an attempt to examine the effect of various precipitation agents such as $KMnO_4$, Na_2CO_3 or KOH, and calcination strategies of the precursors on the physicochemical and catalytic properties of CuMnOx catalyst for CO oxidation. Furthermore, the surface concentration of residual sodium or potassium ions, remaining on the final catalyst surface due to insufficient washing during preparation, also have a poisoning effect on the catalyst [Mirzaei *et al.,* 2003; Njagi *et al.,* 2010]. The enhanced catalytic activity has linked with lower (Na or K)/Mn ratios which was observed for the catalysts produced with longer ageing times. Experiments conducted at a higher pH resulted in the quantity of surface Na^+ or K decreasing and an associated increase in the activity of the system [Jones *et al.,* 2009]. The importance of minimizing the amount of retained Na^+ or K was also important and the presence of sodium or potassium in the final catalyst has been specifically associated to poor activity. When higher ratios of sodium or potassium to copper were detected in the final catalyst, catalytic activity was intensely decreased in all cases. While there have been studies that have focused on ensuring that catalyst poisons, such as Na^+, were absent. The relation between the catalytic activity and the physical characteristics of the catalysts, in terms of particle size, morphology is also discussed in this chapter. The aims of this study to find out the

optimum combination of precipitant apply in the precursor to give the catalyst with highest activity for CO oxidation.

5.1 Experimental

5.1.1 Catalyst preparation

The CuMnOx catalysts were prepared by co-precipitation method and all chemicals used for preparation of catalysts were of analytical grade.

Preparation of CuMnOx catalyst using $KMnO_4$ precipitant

A solution of Manganese acetate $Mn(CH_3COO)_2.4H_2O$ (5.50gm in 20ml H_2O) was added to copper nitrate $Cu(NO_3)_2.3H_2O$ (4.61gm) and stirred for 1h. The mixed solution was taken in the burette and added drop-wise to a solution of $KMnO_4$ (2.37gm in 20ml H_2O) under vigorous stirring conditions for co-precipitation purpose.

Preparation of CuMnOx catalyst using Na_2CO_3 or KOH precipitant

A solution of Manganese acetate $Mn(CH_3COO)_2.4H_2O$ (9.45gm in 20ml H_2O) was added to copper nitrate $Cu(NO_3)_2.3H_2O$ (4.61gm) and stirred for 1h. The mixed solution was taken in the burette and added drop-wise to a solution of KOH or Na_2CO_3 (2.45gm in 20ml H_2O) under vigorous stirring conditions for co-precipitation purpose. The resultant precipitate was stirred continuously for 2h. The precipitate was filtered and washed several times with hot distilled water to remove all the anions. The cake thus obtained was dried at temperature 110^oC for 24h into an oven. The dried precursor thus obtained was divided into three parts for their calcination under three different strategies at 300^oC for 2h.

In the first strategy the precursor was calcined traditionally in a muffle furnace under stagnant air at 300°C for 2h. The second strategy of calcination was under flowing air at a rate of 32.5 $ml.min^{-1}$ at 300°C for 2h. The third strategy of calcination was carried out under reactive mixture of 4.5%CO in air calcination (RC) as follows: Reactive

calcination of the precursor was carried out by the introduction of a low concentration of chemically reactive CO–Air mixture (4.5% CO) at a total flow rate of 32.5 ml.min^{-1} over the hot precursors. After achieving total CO conversion the resultant catalyst was annealed for half an hour at the same temperature then the temperature was increased up to 300^{o}C. The nomenclature of the resulting catalysts thus formed was given by the suffixes '$_{SA}$', '$_{FA}$' and '$_{RC}$' denoting the calcination environment as stagnant air, flowing air or by RC respectively, as depicted in Table 5.1.

Table 5.1: Calcination strategy and nomenclature of the catalysts

Catalyst Name	Calcination Strategy	Nomenclature
CuMnOx precipitate by $KMnO_4$	Stagnant air calcination	$CuMn_{2SA1}$
CuMnOx precipitate by Na_2CO_3		$CuMn_{2SA2}$
CuMnOx precipitate by KOH		$CuMn_{2SA3}$
CuMnOx precipitate by $KMnO_4$	Flowing air calcination	$CuMn_{2FA1}$
CuMnOx precipitate by Na_2CO_3		$CuMn_{2FA2}$
CuMnOx precipitate by KOH		$CuMn_{2FA3}$
CuMnOx precipitate by $KMnO_4$	Reactive calcination	$CuMn_{2RC1}$
CuMnOx precipitate by Na_2CO_3		$CuMn_{2RC2}$
CuMnOx precipitate by KOH		$CuMn_{2RC3}$

5.2 Catalyst Characterization

Characterization of all the $CuMn_2$ catalysts prepared by reactive calcination condition was done by the different techniques and discussed in the following sections. The characterization of the catalysts:

5.2.1 Morphological analysis

The Scanning Electron Micrographs (SEM) instrument was used for the microstructure analysis of the Cu_1Mn_2 catalyst. The SEM micrographs (Figure 5.1) show clearly large differences in the microstructure and morphology of the $CuMn_{2RC}$ catalysts formed by

using different precipitants. They all shows granular particles between 0.5 and 7.8µm calculated by "Image J software" with varying degree of agglomeration as mentioned in Table 5.2. As shown in SEM micrograph, the particles were comprised grains of more coarse, coarse and fine sizes result using, KOH, Na_2CO_3 and $KMnO_4$ precipitants respectively. The SEM result was also in good agreement with XRD analysis. The average particle size of $CuMn_{2RC1,}$ $CuMn_{2RC2}$ and $CuMn_{2RC3}$ catalyst was 0.675µm, 3.127µm and 7.435µm respectively.

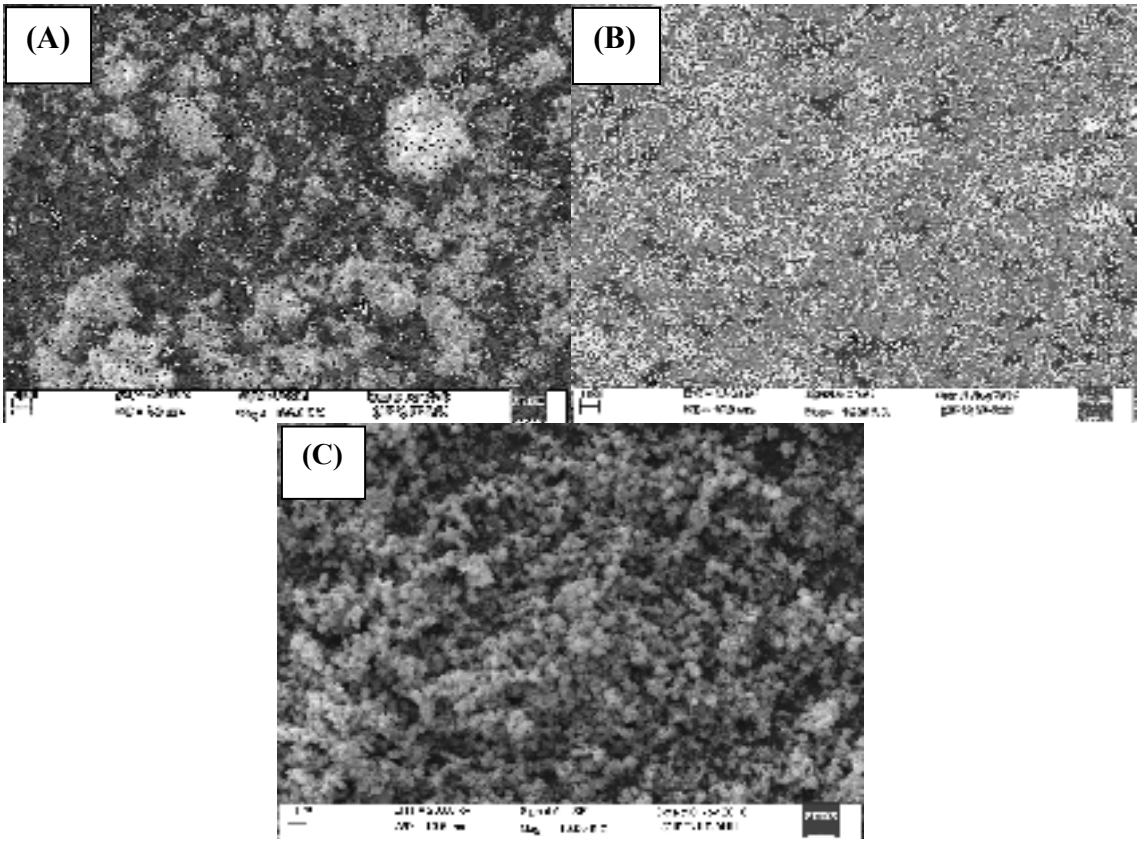

Figure 5.1: Scanning electron micrographs of (A) $CuMn_{2RC3}$, (B) $CuMn_{2RC2}$ and (C) $CuMn_{2RC1}$ catalysts

The particles of $CuMn_{2RC1}$ catalyst was least agglomerated, highly porous, high surface area and uniformly distributed. The choice of various precipitant in the $CuMn_2$ catalysts leads to the change of the surface distribution of Cu, Mn and O elements. The synergetic effect of catalyst was highly depends upon the catalyst composition and nature of oxidized compounds.

Table 5.2: Particle size of $CuMn_{2RC}$ catalysts

Precursor	Catalyst	Particle size (μm)
CuMnOx precipitate by $KMnO_4$	$CuMn_{2RC1}$	0.675
CuMnOx precipitate by Na_2CO_3	$CuMn_{2RC2}$	3.127
CuMnOx precipitate by KOH	$CuMn_{2RC3}$	7.435

All the catalysts have different morphologies, indicating that the types of precipitants used in the precursors have great influence on their catalytic activity. The precipitation of $CuMn_2$ catalyst by small amounts of $KMnO_4$ was more efficient in improving the catalytic behavior for CO oxidation.

5.2.2 Elemental analysis

In order to verify the elemental composition of $CuMn_2$ catalysts, Scanning Electron Microscopy (SEM) with Energy Dispersive X-Ray analysis (SEM-EDX) technique was performed in a large scanning range by random for the samples of $CuMn_{2RC3}$, $CuMn_{2RC2}$ and $CuMn_{2RC1}$ catalysts. The elemental concentration distribution of the catalyst granule was determined by using Isis 300 software. The result of SEM-EDX analysis has shown in the Table 5.3. It can be seen that all the catalyst samples were pure due to the presence of their appropriate elemental peaks only. The different cross-sectioned marks of the $CuMn_{2RC}$ catalysts granules to determine the concentration of different elements located at different cross-section on the catalysts granular surfaces as shown in the Figure 5.2. The presence of Cu, Mn and O on the surface of $CuMn_2$ catalysts can be clearly detected. The atomic ratio and weight ratio of Cu/Mn in the $CuMn_{2RC1}$ catalyst was around 0.558 and 0.567 respectively. The molar ratio of Cu/Mn in all the catalyst samples using co-precipitation method was approximately 0.521, and it was very close to the actual dosage of Cu and Mn presents in the $CuMn_2$ precursors.

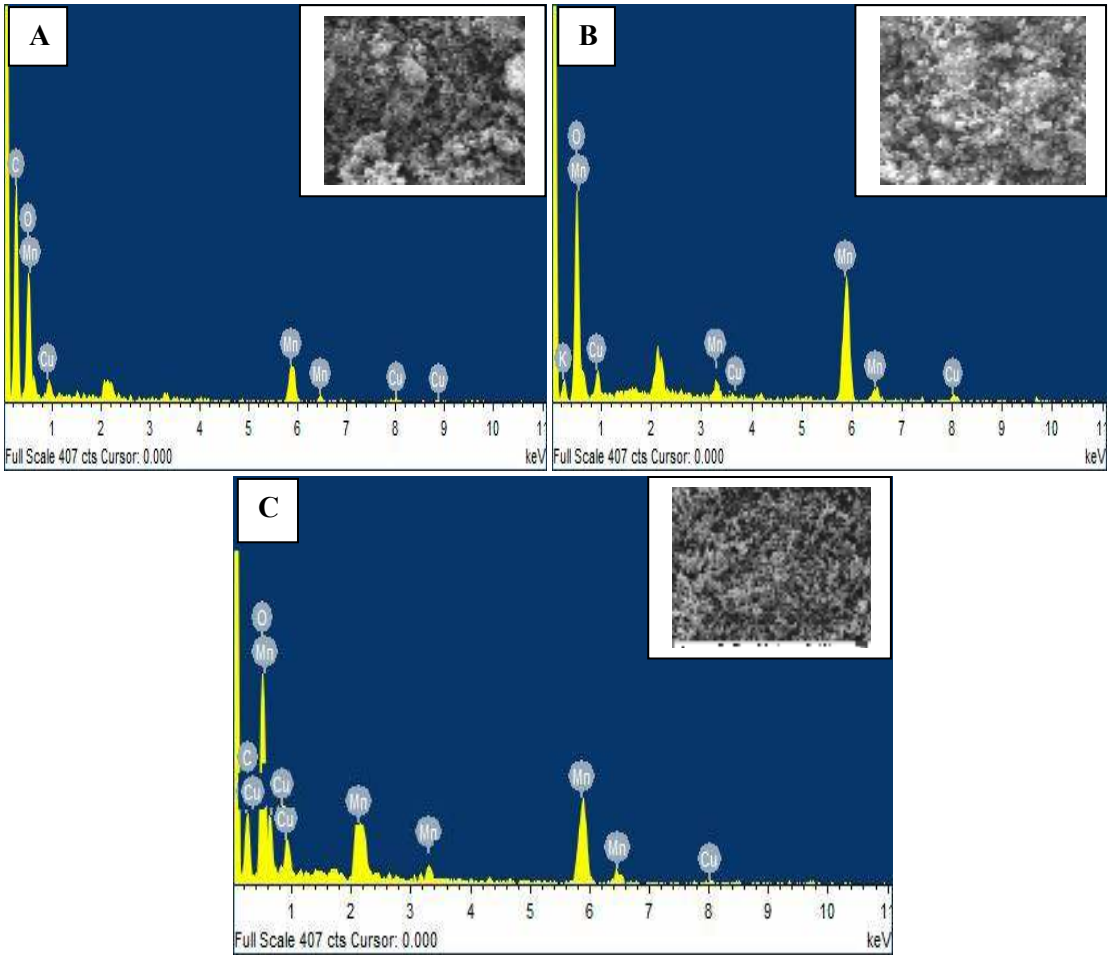

Figure 5.2: SEM-EDX image of (A) $CuMn_{2RC3}$, (B) $CuMn_{2RC2}$ and (C) $CuMn_{2RC1}$ catalysts

The presence of oxygen deficiency in the $CuMn_{2RC1}$ catalyst was least, which makes the high density of active sites. Therefore, it has to shown the best catalytic activity towards CO oxidation. It was clear from the Table 5.3 and Figure 5.2 that the atomic percentage and weight percentage of Mn was also higher as comparison of Cu and O.

Table 5.3: The atomic and weight ratios of Cu, Mn and O in $CuMn_{2RC}$ catalyst by EDX analysis

Catalyst	Atomic ratio (%)				Weight ratio (%)			
	Cu	Mn	O	Cu/Mn	Cu	Mn	O	Cu/Mn
$CuMn_{2RC1}$	30.54	54.65	14.81	0.558	30.81	54.35	14.84	0.567
$CuMn_{2RC2}$	31.65	49.65	18.70	0.637	31.53	50.58	17.89	0.623
$CuMn_{2RC3}$	32.29	47.95	19.76	0.673	32.38	46.91	20.71	0.690

A calcination of the $CuMn_{2RC}$ catalyst was highly influenced the elemental distribution of different elements presents on the surface of catalysts. The choice of different precipitant leads to the change of surface distribution of Cu, Mn and O elements, which might be related to the CO oxidation.

5.2.3 Phase identification and cell dimensions

The phase identification and cell dimensions of $CuMn_2$ catalysts prepared in reactive calcination conditions were done by the X-ray powder diffraction (XRD) technique. It was carried out to evaluate the crystallite size and coordinate dimensions present in the surface layer of catalysts. XRD patterns of the $CuMn_2$ catalyst produced by reactive calcination of the precursors using three different precipitants of $KMnO_4$, Na_2CO_3 or KOH were displayed in Figure 5.3. XRD pattern of the $CuMn_{2RC1}$ catalyst has shown that the diffraction peak at 2θ of 36.96 corresponds to Face-centered cubic $Cu_1Mn_2O_4$ (PDF-35-1174 JCPDS file). The crystallite size of the catalyst determined by the Scherrer eq^n. (2.3.1) was 3.90 nm. In $CuMn_{2RC2}$ catalyst has shown that the diffraction peak at 2θ of 37.04 corresponds to End-centered cubic CuO (PDF-45-0937 JCPDS file) and Mn_2O_3 (PDF-33-0900 JCPDS file) mixture with crystallite size of 4.24 nm.

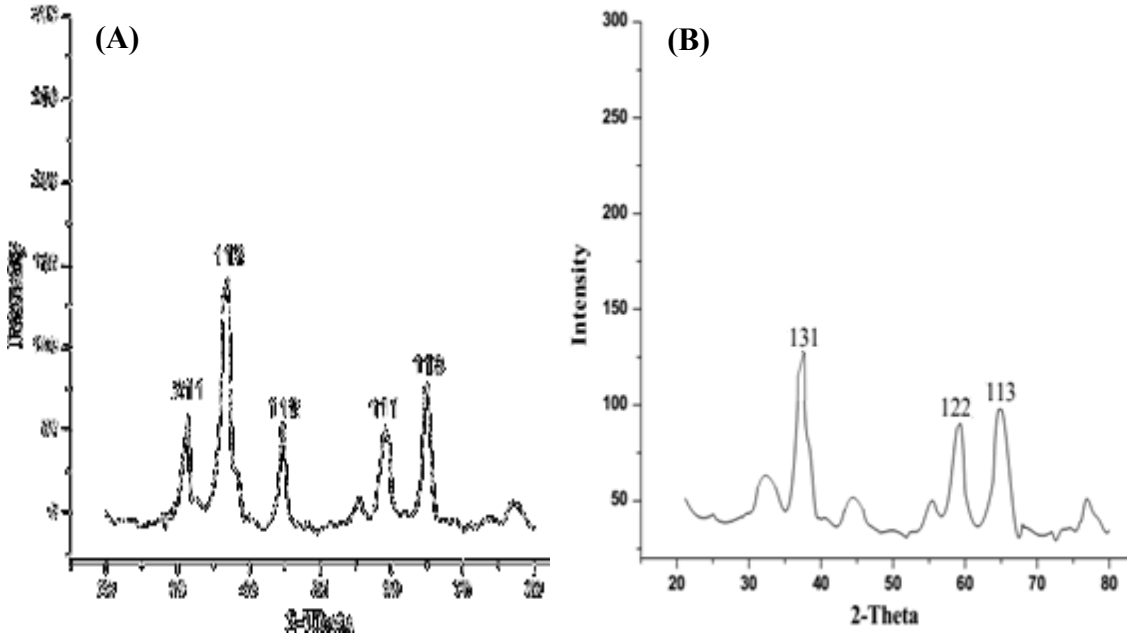

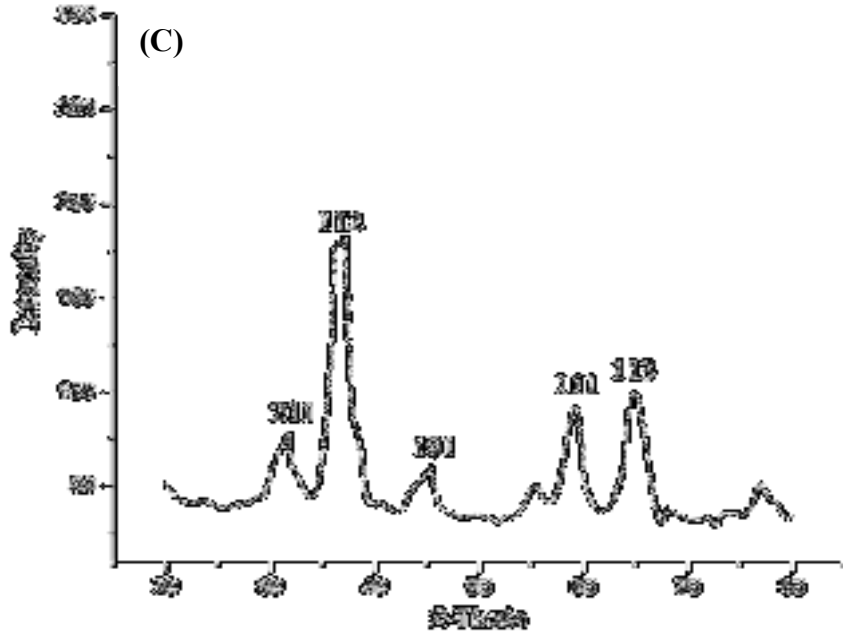

Figure 5.3: XRD analysis of (A) $CuMn_{2RC1}$, (B) $CuMn_{2RC2}$ and (C) $CuMn_{2RC3}$

The structure, phase and crystallite size was also discussed in Table 5.4. The XRD pattern of $CuMn_{2RC3}$ catalyst was shown that the diffraction peak at 2θ of 37.37 corresponds to Face-centered cubic $Cu_1Mn_2O_4$ (PDF-35-1174 JCPDS file). The crystallite size of catalyst was 5.26 nm.

Table 5.4: XRD analysis of $CuMn_{2RC}$ catalysts

Catalyst	Structure	Phase	Crystallite size
$CuMn_{2RC1}$	Face-centered cubic	$Cu_1Mn_2O_4$	3.90nm
$CuMn_{2RC2}$	End-centered cubic	CuO, Mn_2O_3	4.24nm
$CuMn_{2RC3}$	Face-centered cubic	$Cu_1Mn_2O_4$	5.26nm

The order of crystallite size in descending order present in the catalysts obtained by RC conditions was as follows: $CuMn_{2RC3}$> $CuMn_{2RC2}$> $CuMn_{2RC1.}$ The crystallites form produced by the RC of $CuMn_{2RC1}$ catalyst exhibited smallest size (3.90nm) in comparison to $CuMn_{2RC2}$ (4.24 nm) and $CuMn_{2RC3}$ (5.265nm) catalyst. Finally, it confirmed that the particles present in $CuMn_{2RC1}$ catalyst was most crystalline form,

and producing narrow size high-intensity diffraction lines; as compared to other catalysts. After XRD analysis we can confirmed that the crystallite size of $CuMn_{2RC1}$ has lower than the $CuMn_{2RC2}$ and $CuMn_{2RC3}$ catalysts. The $CuMn_{2RC1}$ and $CuMn_{2RC2}$ catalysts prepared with ($KMnO_4$ and KOH) as a precipitant however mainly have a spinel $Cu_{1.5}Mn_{1.5}O_4$ structure was observed following calcination at 300^oC. The refinement of XRD pattern of the $CuMn_{2RC}$ has shows that there will be no impurity phases were present in the catalysts. The different types of precipitants can influence the final crystalline phases of the catalysts [Cai *et al.,* 2012].

5.2.4 Identification of materials present in a catalyst

The FTIR transmission spectrum of the $CuMn_{2RC1}$, $CuMn_{2RC2}$ and $CuMn_{2RC3}$ catalysts prepared by reactive calcination (RC) conditions has shown in the Figure 5.4. In $CuMn_{2RC1}$ catalyst at the transmittance conditions, there are total three peaks obtained, the IR band 1640cm^{-1} showed the presence of MnO_2 group, -OH group is showed at 3490cm^{-1} and wave number 1180cm^{-1} is showed CuO group. In $CuMn_{2RC2}$ catalyst at the transmittance conditions, there are total four peaks obtained, the IR band 1640cm^{-1} has shown the presence of Mn_2O_3 group, 3490cm^{-1} is showed -OH group, 1180cm^{-1} is showed CuO group and 2140cm^{-1} is showed CO_3^{2-} group [Cai *et al.,* 2012].

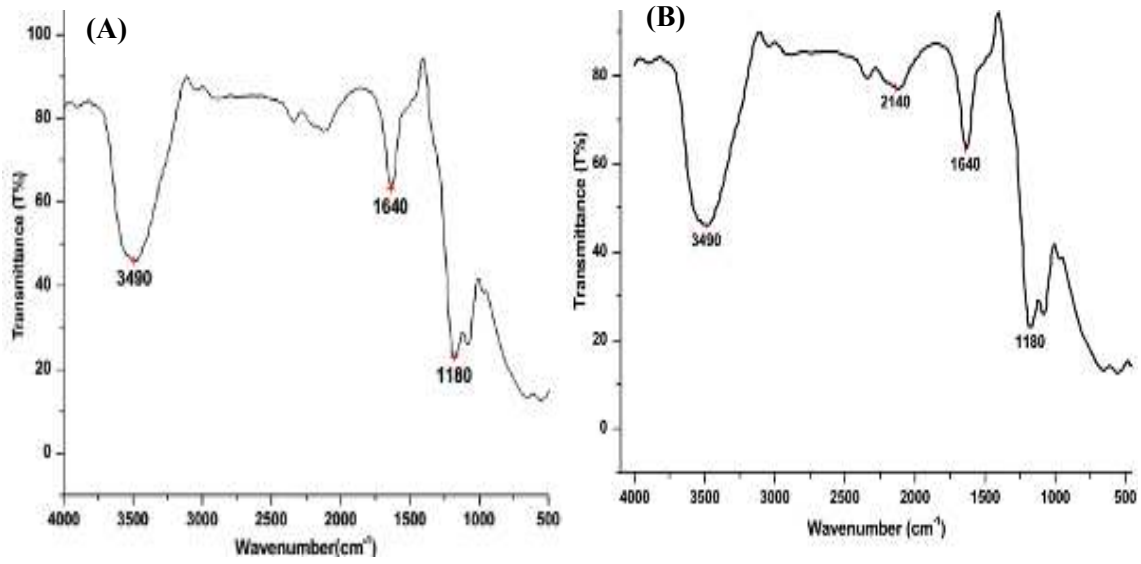

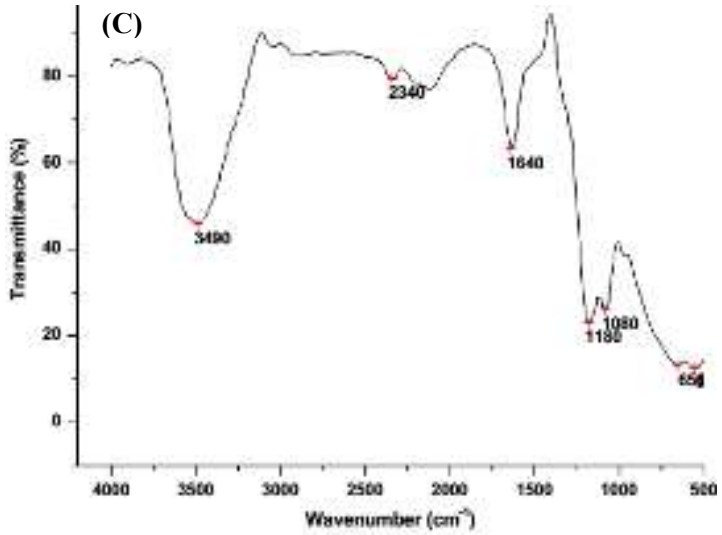

Figure 5.4: FTIR analysis of (A) $CuMn_{2RC1}$, (B) $CuMn_{2RC2}$ and (C) $CuMn_{2RC3}$ catalysts

In $CuMn_{2RC3}$ catalyst, there are total six peaks obtained, the IR band 1640cm^{-1} has shown the presence of MnO_2 group, 3490cm^{-1} -OH group, 1180cm^{-1} CuO group, 2340cm^{-1} Mn_2O_3 group. The other phases like C-O-C group and C=O group are present at 1080cm^{-1} and 656cm^{-1} respectively [Adánez-Rubio *et al.,* 2017]. The FTIR analysis shows that the $CuMn_{2RC1}$ catalyst was free from the impurity; therefore, the activity of the catalyst has been increased. All the catalysts; this originates from the stretching vibrations of the metal-oxygen bonds and confirmed the presence of CuO and MnO_2 phases. The weak band at 1180cm^{-1} indicates that the presence of some CO_3^{2-} group in the catalysts. The spectra of impurities decrease in the following order: $CuMn_{2RC3}$ > $CuMn_{2RC2}$ > $CuMn_{2RC1}$. Thus the $CuMn_{2RC1}$ catalyst has shown the highest purity as compared to other catalysts. The adsorption strength and adsorption capacity of CO on the catalyst surfaces depends upon the uniform degree of dispersion of Cu and Mn components. When the adsorption capacity is moderate, thereby good catalytic activity exhibited [Guo *et al.,* 2016].

5.2.5 Identification and quantification of elements

The surface valence state and quantification of elements were investigated by the X-ray photoelectron spectroscopy (XPS) analysis. The XPS analysis was mainly used to understand the physical and chemical changes of catalysts by exposure of gaseous molecules under different thermal conditions have been examined. Although it can be proposed that the high binding energy was preferably for CO oxidation. Below figures display the XPS spectra in the Cu(2p), Mn(2p) and O(1s) regions present in the $CuMn_{2RC}$ catalysts. The prominent peak of Cu(2p) level in $CuMn_{2RC1}$, $CuMn_{2RC2}$ and $CuMn_{2RC3}$ catalyst was deconvoluted into six peaks centered. By performing peak fitting deconvolution of the main Cu(2p) in all calcination catalyst was Cu(II) oxide form.

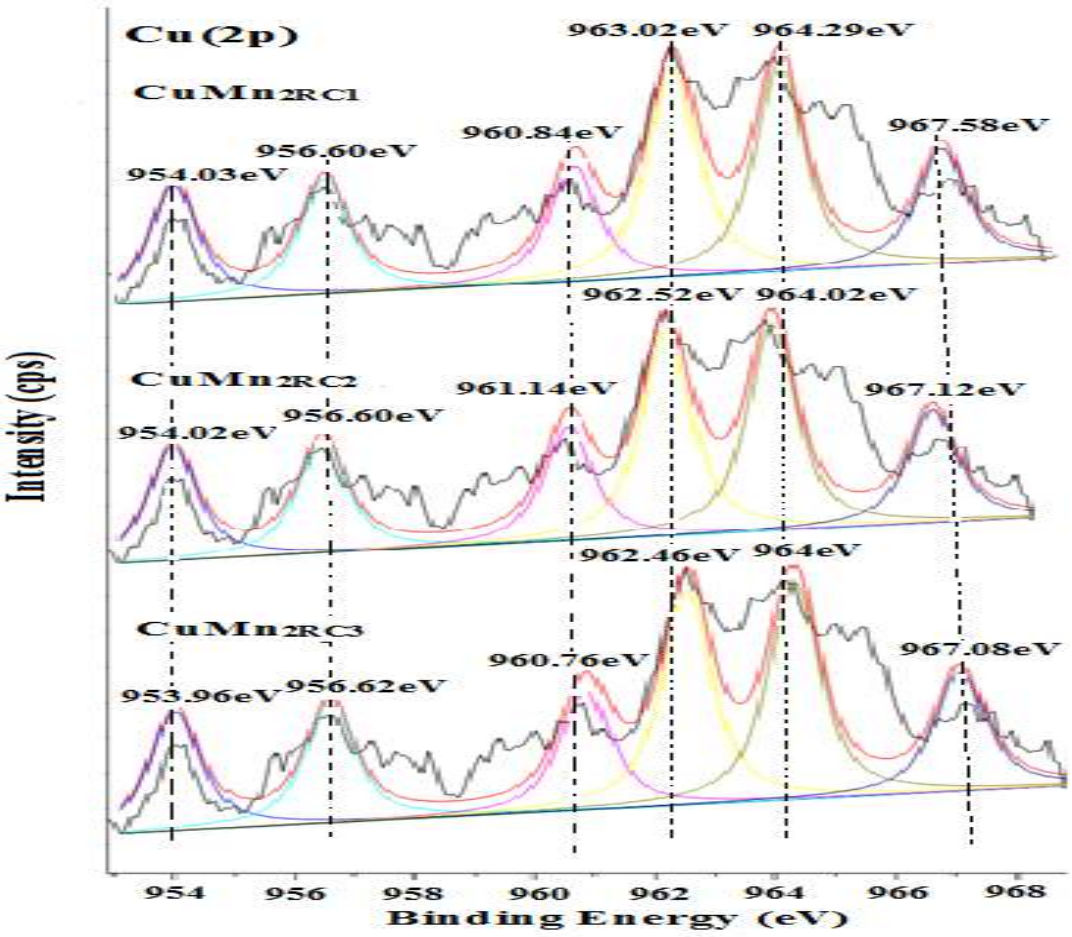

Figure 5.5: XPS analysis of Cu(2p) in $CuMn_{2RC}$ catalysts

The binding energy of Cu(2p) in $CuMn_{2RC1}$ catalyst was 954.03eV, 956.60eV, 960.84eV, 963.02eV, 964.29eV and 967.58eV and $CuMn_{2RC2}$ catalyst was 954.02eV, 956.60eV, 961.14eV, 962.52eV, 964.02eV and 967.12eV and $CuMn_{2RC3}$ catalyst was 953.96eV, 956.62eV, 960.76eV, 962.46eV, 964eV and 967.08eV. The highest intensuty peak of Cu(2p) in $CuMn_{2RC1}$, $CuMn_{2RC2}$ and $CuMn_{2RC3}$ catalyst was 964.29eV, 964.02eV and 964eV respectively. It was clear from Figure 5.5 that the binding energy of Cu(2p) in $CuMn_{2RC1}$ catalyst was highest as comparison of other catalysts. Figure 5.6 and 5.7 represents the prominent peak of Mn(2p) and O(1s) level in $CuMn_{2RC}$ catalyst was deconvoluted into double peak. By performing peak fitting deconvolution of the main Mn(2p) in all catalysts can be divided into two components including Mn^{4+} and Mn^{3+}. Since the difference between the binding energy values of Mn^{3+} and Mn^{4+} ions are small. The binding energy of Mn(2p) in $CuMn_{2RC1}$, $CuMn_{2RC2}$, and $CuMn_{2RC3}$ catalysts at reactive calcination condition is (643.24eV and 656.15eV), (643.16eV and 656.12eV) and (643.08eV and 656.10eV) respectively and it will be associated with the presence of Mn^{3+}, Mn^{4+} and satellite in all samples.

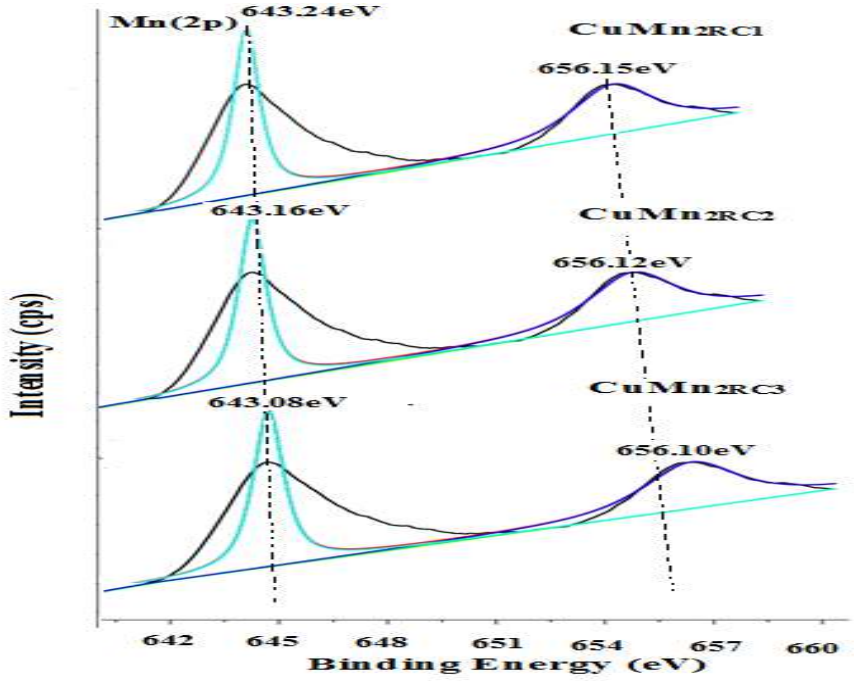

Figure 5.6: XPS analysis of Mn(2p) in $CuMn_{2RC}$ catalysts

From Figure 5.6, we have observed that the wide-ranging Mn^{4+} peak presents in $CuMn_{2RC1}$ catalyst was higher than $CuMn_{2RC2}$ and $CuMn_{2RC3}$ catalyst. The highest binding energy peak of Mn(2p) in $CuMn_{2RC1}$, $CuMn_{2RC2}$, and $CuMn_{2RC3}$ catalyst at reactive calcination condition was 656.15eV, 656.12eV and 656.10eV respectively. The binding energy of Mn(2p) in $CuMn_{2RC1}$ catalyst was highest as compared to $CuMn_{2RC2}$ and $CuMn_{2RC3}$ catalysts. The binding energy of O(1s) was displayed in Figure 5.7. Generally, there are two different types of oxygen present in the catalysts with the binding energy of (529.2–530eV) and (531.3–532.2eV), which could be recognized as chemisorbed oxygen and lattice oxygen respectively.

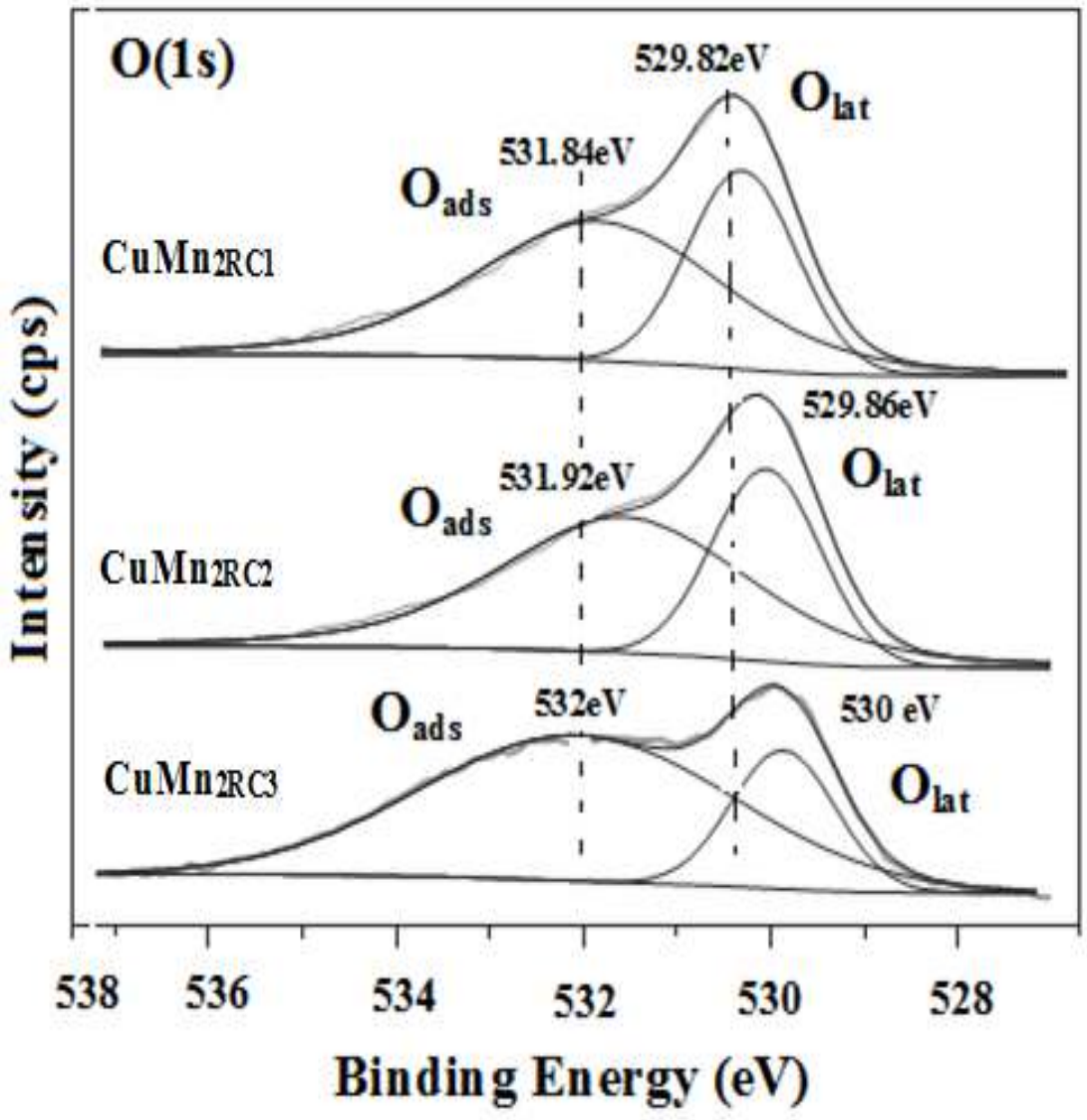

Figure 5.7: XPS analysis of O(1s) in the catalysts

In present study, the oxygen with the binding energy of 529.82eV was the main form and could be recognized as the chemisorbed oxygen (Oa). The binding energy of O(1s) in $CuMn_{2RC1}$, $CuMn_{2RC2}$ and $CuMn_{2RC3}$ catalyst was (531.84eV and 529.82eV), (531.92eV and 529.86eV) and (532eV and 530eV) respectively. The presence of lattice oxygen was very small in $CuMn_{2RC1}$ catalyst. In this case, the oxygen with the binding energy of 531.78eV was the main form and could be assigned to the chemisorbed oxygen (Oa). The presence of lattice oxygen was very small in $CuMn_{2RC1}$ catalyst. Table 5.5 represents the chemical state and binding energy of $CuMn_{2RC}$ catalysts prepared in reactive calcination conditions. It was confirmed that $Mn(CH_3COO)_2.4H_2O$ usually decomposed into MnO_2 form and $Cu(NO_3)_2.3H_2O$ usually decomposed into Cu(II)Oxide form after reactive calcination conditions. The binding energy of $CuMn_{2RC1}$ catalyst was highest as comparison of $CuMn_{2RC2}$ and $CuMn_{2RC3}$ catalysts.

Table 5.5: Binding energy and chemical state of $CuMn_{2RC}$ catalysts

Sample	**Elements**		
	Cu	**Mn**	**O**
$CuMn_{2RC1}$	Cu(II) Oxide 964.29eV	MnO_2 643.24eV	C-O 529.82eV
$CuMn_{2RC2}$	Cu(II) Oxide 964.02eV	MnO_2 643.16eV	C-O 529.86eV
$CuMn_{2RC3}$	Cu(II) Oxide 964eV	MnO_2 643.08eV	C-O 530eV

One of noticeable fact was that the amount of oxygen presents less in reactive calcined prepared $CuMn_{2RC1}$ catalyst as compared to $CuMn_{2RC2}$ and $CuMn_{2RC3}$ catalyst, due to an absence of lattice oxygen which can creates the oxygen vacancies for CO oxidation. The content order of $O_a/(O_a+O_l)$ ratio was shown as follows: $CuMn_{2RC1}$> $CuMn_{2RC2}$>

$CuMn_{2RC3}$. The presence of higher oxidation state phases could be the result of a greater degree of surface interaction between the easily oxidisable manganese phase and highly reducible copper phase. The huge amount of surface chemisorbed oxygen (most active oxygen) was preferable for improving the catalytic activity for CO oxidation. The extraordinary performance of $CuMn_{2RC1}$ catalyst produced by RC in CO oxidation was associated with their characterizations such as physical and chemical changes, binding energy and oxygen deficient defective structure which can create the high density of active sites. In addition, the interaction between Cu and Mn phases during decomposition facilitates the formation of stable metal oxide interfaces. These XPS results suggest that the most active $CuMn_{2RC1}$ catalyst had a relatively higher amount of lower valence manganese and loosely bound lattice oxygen. The XPS spectra show the carbon peak C(1s) at 285eV (Binding energy).

The satellite features at 643eV higher binding energy from the main peaks that are a fingerprint of the presence of MnO_2. XPS also indicates that there is neither Na nor K signals in all these samples, thus inferring the purity of the samples with respect to the starting reagents. The full width at half maximum (FWHM) values suggests one of the possible reasons for these high values was line broadening resulting from multiple splitting. The XPS results indicate that at least some of the Cu^{2+} phase was predominantly in the catalysts surface. The Cu^{+} cations have been proposed to appear in the $CuMn_{8RC}$ catalyst as a consequence of redox equilibrium between Cu^{2+}/Cu^{+} and Mn^{3+}/Mn^{4+} in an amount which depends on the temperature of the thermal treatment employed for its preparation. With the help of XPS analysis we can determination the oxidation state of elements on the surfaces.

5.2.6 Surface area measurement

The surface area of $CuMn_{2RC}$ catalyst was prepared by the co-precipitation method with a new route of reactive calcination conditions is measured by BET technique. The isotherm gave valuable information on the meso-pore structure through its hysteresis loop. The prepared samples exhibited hysteresis loop, which indicated that the pores were exhibiting geometries of meso-pores. The effect of precipitation agents on the isotherms of $CuMn_{2RC}$ catalyst has shown in the Figure 5.8. It can be visualized from the Table 5.6 that the pore volume and pore size of $CuMn_{2RC1}$ catalyst in reactive calcined was very much superior to the other catalysts.

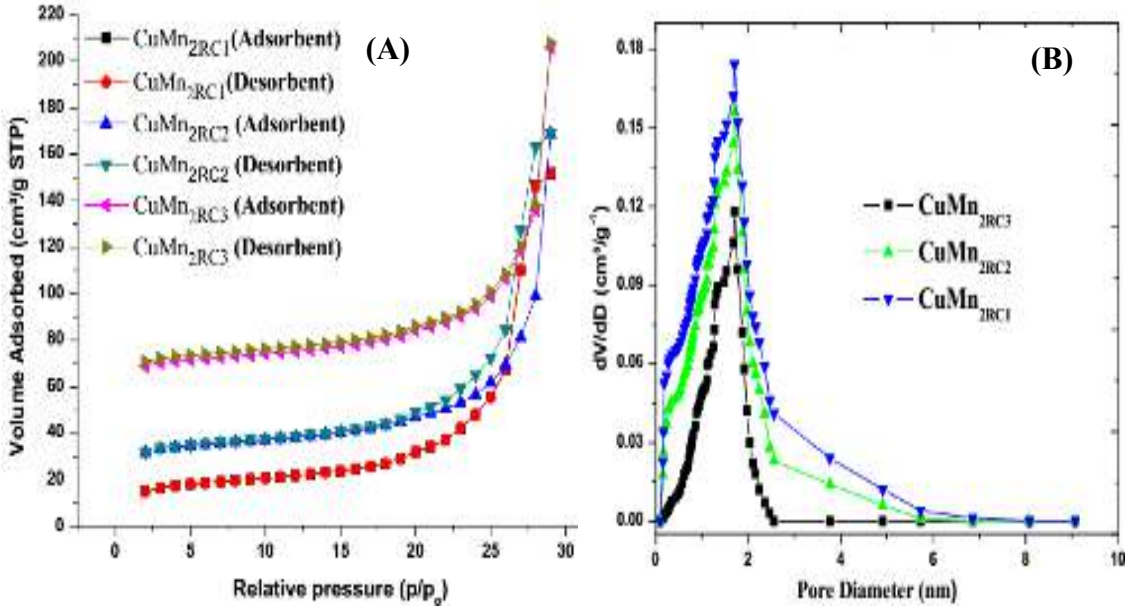

Figure 5.8: Textural properties (A) N_2 adsorption-desorption isotherms and (B) Pore size distributions curves

A hysteresis loop at a relative pressure (P/P_0) of 0.8–1.0 indicates that the porosity arising from the non-crystalline intra-aggregate voids and spaces formed by the inter-particle contacts. Figure 5.8 shows that the pore size distributions (PSDs) as calculated by the Barrett–Joyner–Halendar (BJH) method from the desorption branch of the nitrogen isotherms. The porous textural parameters, such as specific surface area (S_{BET})

and pore volume (V_{total}) were also listed in the Table 5.6. The surface area of $CuMn_{2RC1}$, $CuMn_{2RC2}$ and $CuMn_{2RC3}$ catalyst was 118.24, 102.15 and 93.45m^2/g respectively. These data clearly indicates that the precipitant present in precursor has a high efficacy for low-temperature CO oxidation. Specific surface area and total pore volume were two significant factors which can affects the catalytic activity for CO oxidation.

Table 5.6: Textural property of $CuMn_{2RC}$ catalysts

Catalyst	**Surface Area (m^2/g)**	**Pore Volume (cm^3/g)**	**Ave. Pore Size (Å)**
$CuMn_{2RC1}$	118.24	0.627	54.55
$CuMn_{2RC2}$	102.15	0.545	65.30
$CuMn_{2RC3}$	93.45	0.429	74.55

The specific surface area was measured by BET analysis and it was also follows the SEM and XRD results. The catalyst surface area of similar magnitude regardless of the preparation atmosphere; however, there was a general increase in surface area as a result of choosing suitable precipitant. The average pore diameter increase with the increasing of calcination temperature because a high-temperature treatment led to the particle sintering accompanied with a loss in the active area. A large number of more pores present in a catalyst surface mean a higher number of CO molecules were trapped on their surfaces, it causes better catalytic activity.

5.3 Catalyst performance and activity measurement

Activity test of the catalyst was carried out to evaluate the effectiveness of $CuMn_2$ catalysts as a function of temperature. It was evaluated in different calcination conditions like stagnant air, flowing air and reactive calcination. An activity was

increased with the increasing of temperature from room temperature to certain high temperature for full conversion of CO. The activity of $CuMn_2$ catalysts, produced by co-precipitation method using different types of precipitants, for CO oxidation was discussed in below. The light-off characteristics were used to evaluate the activity of resulting catalysts with the increasing of temperature.

5.3.1 Activity of $CuMn_{2SA}$ catalysts produced under stagnant air calcination

The activity of the $CuMn_{2SA}$ catalysts prepared in stagnant air calcination conditions for CO oxidation was done in the laboratory. CO conversion Vs temperature over different catalyst is plotted in Fig. 5.9 and the light off characteristics of the catalysts is given in Table 5.7.

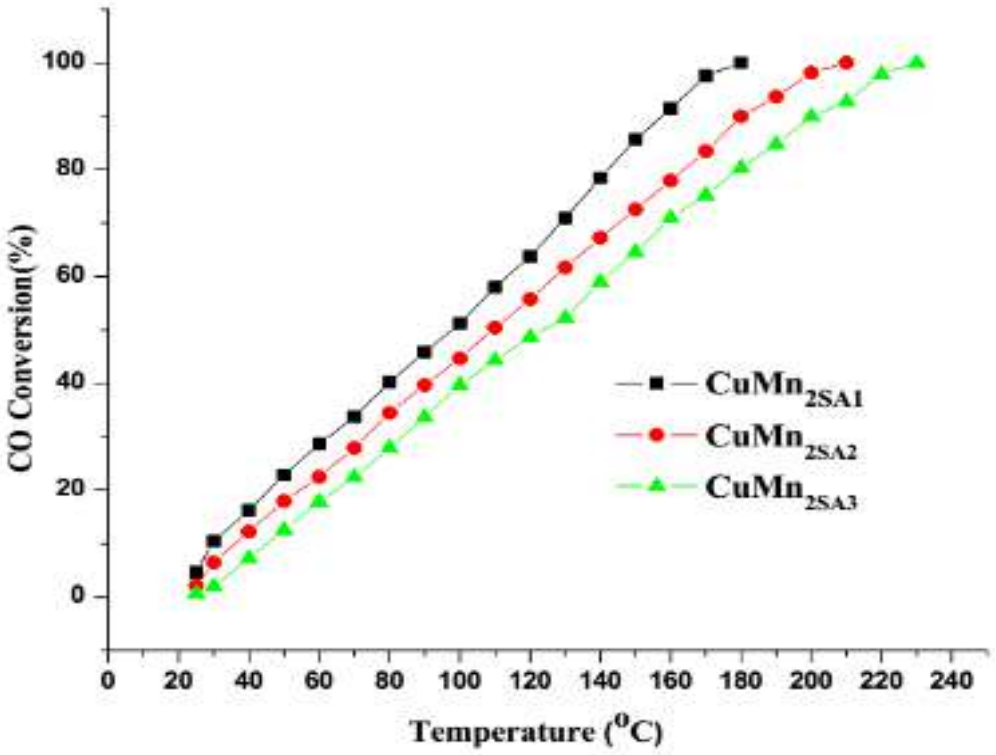

Figure 5.9: Catalytic activity of various $CuMn_{2SA}$ catalysts for CO oxidation

It is evident from the Figure 5.9 and Table 5.7 that the oxidation of CO was initiated (T_{10}) over the $CuMn_{2SA1}$, $CuMn_{2SA2}$ and $CuMn_{2SA3}$ at different temperatures of 30°C, 38°C and 62°C respectively. The 50% conversion of CO was occurred at 100ºC over

$CuMn_{2SA1}$ catalyst, which was less by 10ºC and 35ºC over than that of $CuMn_{2SA2}$ and $CuMn_{2SA3}$ catalyst respectively. The total oxidation temperature of CO was 180ºC for $CuMn_{2SA1}$, which was less by 30ºC and 50ºC over than that of $CuMn_{2SA2}$ and $CuMn_{2SA3}$ catalysts respectively. After the activity test we have observed that the $CuMn_{2SA1}$ catalyst has shown the best catalytic activity for CO oxidation at a low temperature as compared to the other catalysts.

Table 5.7: Light-off characteristics of $CuMn_{2SA}$ catalysts

Catalyst	**T_{10}**	**T_{50}**	**T_{100}**
$CuMn_{2SA1}$	30ºC	100ºC	180ºC
$CuMn_{2SA2}$	38ºC	110ºC	210ºC
$CuMn_{2SA3}$	62ºC	135ºC	230ºC

The activity order of each catalyst for total oxidation of CO was in accordance with their characterization. The order of activity of different types of $CuMn_2$ catalysts for CO oxidation was as follows: $CuMn_{2SA1}$> $CuMn_{2SA2}$> $CuMn_{2SA3}$. Using the same precursor, the catalysts prepared with $KMnO_4$ as the precipitant was considerably more active than the catalysts prepared with Na_2CO_3 or KOH as the precipitant. The coordination between $CuMn_2$ precursor and the appropriate precipitate ($KMnO_4$) was an improving the activity of catalysts for CO oxidation.

5.3.2 Activity of $CuMn_{2FA}$ catalysts produced under flowing air calcination

The copper nitrate and manganese acetate most widely used as a precursors in the preparation of various catalysts. The individual property of copper nitrate and manganese acetate in $CuMn_{2FA}$ precursors has also an effect on the activity of resulting

catalyst. In the initial conditions, a very slow exothermic reaction for CO oxidation was going on over the catalyst, it causes rising in the local temperature. The increased in local temperature will decreased the decomposition of the precursor. The oxidation of CO has initiated in flowing air calcination conditions over the $CuMn_{2FA1}$, $CuMn_{2FA2}$ and $CuMn_{2FA3}$ were 25°C, 30°C and 40°C respectively and the 50% conversion of CO over the $CuMn_{FA1}$ catalyst was 70°C, which was less by 10°C and 30°C over than that of $CuMn_{FA2}$ and $CuMn_{FA3}$ catalysts respectively.

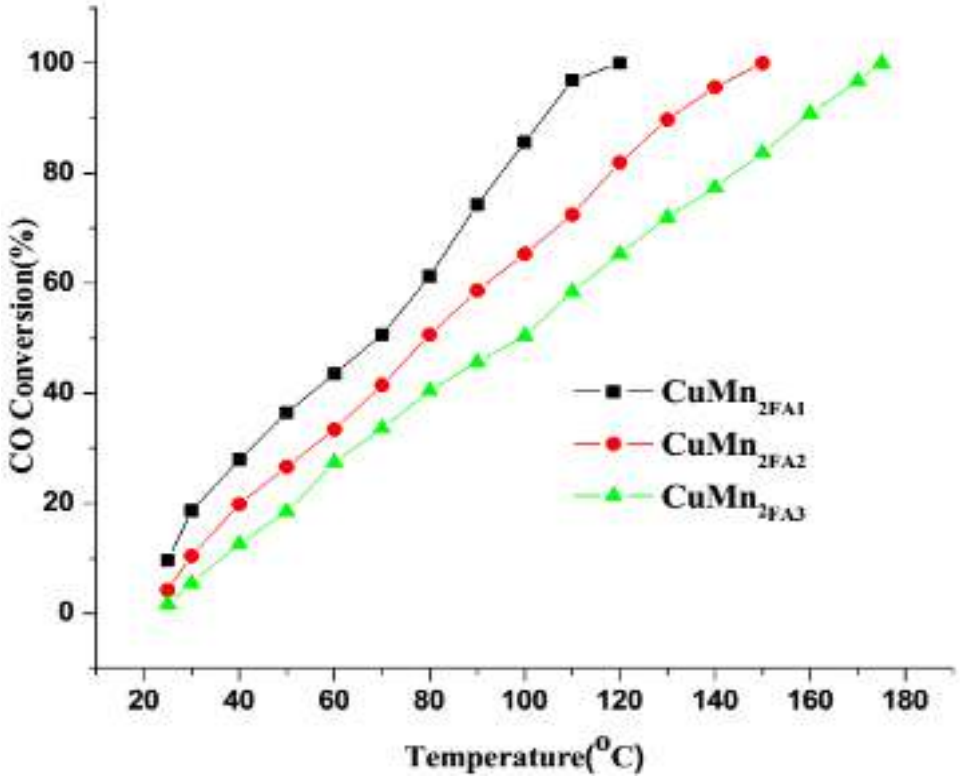

Figure 5.10: Catalytic activity of various $CuMn_{2FA}$ catalysts for CO oxidation

The total oxidation temperature of CO was 120ºC for $CuMn_{2FA1}$ catalyst, which was less by 30°C and 55°C over than that of $CuMn_{2FA2}$ and $CuMn_{2FA3}$ catalysts respectively. Activity of the catalysts seems to be dominated both by their average oxidation number and the presence of different element species in a catalyst surfaces. The order of activity of different types of $CuMn_{2FA}$ catalysts for CO oxidation was as follows: $CuMn_{2FA1}$> $CuMn_{2FA2}$> $CuMn_{2FA3}$. After the activity test, we can confirm that the $CuMn_{2FA1}$ catalyst has a higher catalytic activity for CO oxidation, as compared to

the other catalysts. This experimental results shows that the effect of precipitation agents such as Na_2CO_3, $KMnO_4$ or KOH on the precursors of $CuMn_2$ catalyst for CO oxidation.

Table 5.8: Light-off characteristics of $CuMn_{2FA}$ catalysts

Catalyst	T_{10}	T_{50}	T_{100}
$CuMn_{2FA1}$	25ºC	70ºC	120ºC
$CuMn_{2FA2}$	30ºC	80ºC	150ºC
$CuMn_{2FA3}$	40ºC	100ºC	175ºC

The $CuMn_2$ catalysts prepared with $KMnO_4$ as the precipitant shows the best catalytic activity for CO oxidation at a lower temperature. It was found that the precipitant could lead to different crystalline phase formation of the catalysts. The preparation of catalysts was highly influence their structure and activity. As compared to stagnant air calcination, the flowing air produced more active catalysts for CO oxidation at a low temperature. The order of activity of catalysts calcined under flowing air (FAC) was higher than that of stagnant air (SAC) i.e.: FAC > SAC.

5.3.3 Activity of $CuMn_{2RC}$ catalysts produced under reactive calcination

The reactive calcination (RC) conditions not only minimized a process step but also produced $CuMn_{2RC}$ catalysts with improved performance for CO oxidation. The oxidation of CO was initiated over the $CuMn_{2RC1}$, $CuMn_{2RC2}$ and $CuMn_{2RC3}$ were 22°C, 26°C and 30°C respectively and 50% conversion of CO over the $CuMn_{2RC1}$ catalyst was 45°C, which was less by 10°C and 30°C over than that of $CuMn_{2RC2}$ and $CuMn_{2RC3}$ catalysts respectively. The total oxidation temperature of CO was 80ºC for $CuMn_{2RC1}$ catalyst, which was less by 20°C and 35°C over than that of $CuMn_{2RC2}$ and $CuMn_{2RC3}$ catalysts respectively.

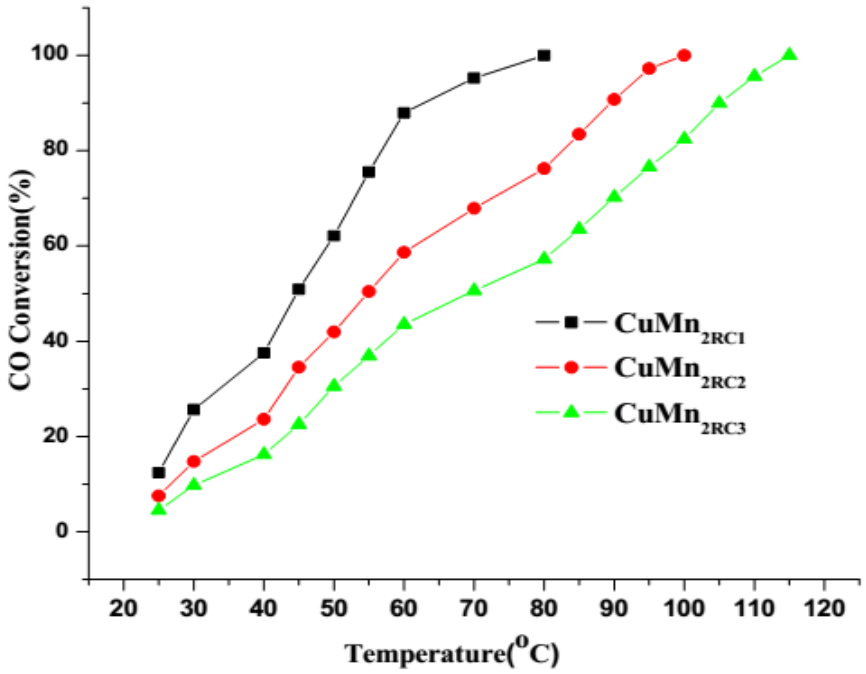

Figure 5.11: Catalytic activity of various $CuMn_{2RC}$ catalysts for CO oxidation

It was clear from the Table 5.9 and Figure 5.11 that the $CuMn_{2RC1}$ has shown the best catalytic activity for CO oxidation as compared to the other catalysts. The order of activity of different types of $CuMn_{2RC}$ catalysts for CO oxidation was as follows: $CuMn_{2RC1}$> $CuMn_{2RC2}$> $CuMn_{2RC3}$.

Table 5.9: Light-off characteristics of $CuMn_{2RC}$ catalysts

Catalyst	T_{10}	T_{50}	T_{100}
$CuMn_{2RC1}$	22ºC	45ºC	80ºC
$CuMn_{2RC2}$	26ºC	55ºC	100ºC
$CuMn_{2RC3}$	30ºC	75ºC	115ºC

The order of activity of various calcination conditions was as follows: RC > FAC > SAC. After the activity test, we can confirm that the $CuMn_{2RC1}$ catalyst has a higher catalytic activity for CO oxidation as compared to the other catalysts. Therefore, the

$CuMn_{2RC1}$ catalyst has shown the promising performance for CO oxidation at a low temperature and these systems were now worthy for further investigation.

5.3.4 Comparison of reactive calcination with traditional calcination

The RC route was the most appropriated calcination strategy for the production of highly active $CuMn_2$ catalyst (precipitate by $KMnO_4$) for CO oxidation. A comparative study of CO oxidation over the ($CuMn_{2SA1}$, $CuMn_{2FA1}$ and $CuMn_{2RC1}$) catalysts produced under various calcination conditions of stagnant air, flowing air and RC has shown in the Figure 5.12. The calcination strategies have a drastic effect on the activity of resulting catalyst. The oxidation of CO has just initiated at room temperature ~25°C overall all the catalyst samples and 50% conversion of CO over the $CuMn_{2RC1}$ was 45°C, which was less by 25°C and 55°C over than that of $CuMn_{2FA1}$ and $CuMn_{2SA1}$ respectively.

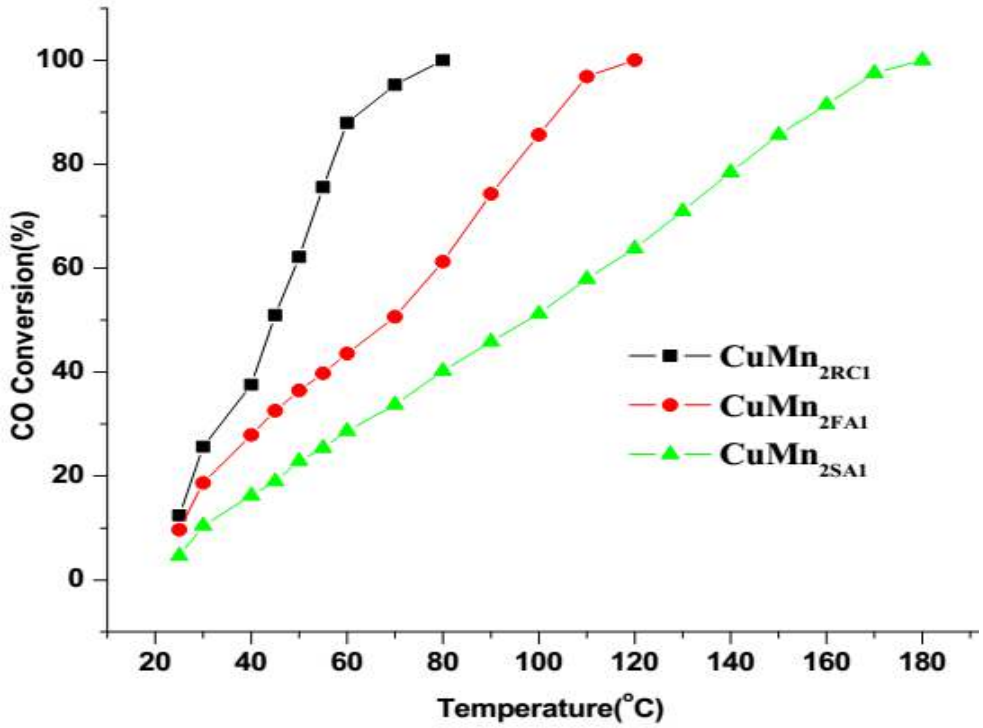

Figure 5.12: Activity test of $CuMn_2$ catalysts under various calcination conditions

The total conversion temperature of CO was 80ºC for $CuMn_{2RC1}$ catalyst, which was less by 40°C and 100°C over than that of $CuMn_{2SA1}$ and $CuMn_{2FA1}$ catalysts respectively. The activity order of CO oxidation in the decreasing sequence was in accordance with their characterization by SEM-EDX, BET, XRD, XPS and FTIR as follows: $CuMn_{2RC1}$> $CuMn_{2FA1}$> $CuMn_{2SA1}$. The improved catalytic activity of reactive calcination can be ascribed to the unique structural and textural characteristics as the smallest crystallites of $CuMn_{2RC1}$. The highest activity of the $CuMn_{2RC1}$ catalyst was associated with the creation of smallest crystallites authenticated by XRD observation.

Table 5.10: Light-off characteristics of $CuMn_2$ (precipitate by $KMnO_4$) catalysts

Catalyst	**T_{10}**	**T_{50}**	**T_{100}**
$CuMn_{2SA1}$	25ºC	100ºC	180ºC
$CuMn_{2FA1}$	25ºC	70ºC	120ºC
$CuMn_{2RC1}$	25ºC	45ºC	80ºC

The result obtained in this work has shown that the precipitants had a significant impact on the crystalline phases of the catalysts for CO oxidation. The results from XRD, FTIR and BET measurements propose strongly that the crystalline phase of dried samples prepared with various types of precipitants were all different despite being synthesized with the same precursors. The $CuMn_{2RC}$ catalyst synthesized using $KMnO_4$ (precipitant) by RC conditions has shown that the best catalytic activity for CO oxidation. Using the same precursor, the catalysts prepared with Na_2CO_3 as the precipitant were considerably more active than catalysts prepared with KOH as the precipitant. The combination of precipitant and precursor in the precipitation process plays an important role in producing the high catalytic activity.

5.4 Concluding Remarks

$CuMn_2$ have been prepared using different precipitants ($KMnO_4$, Na_2CO_3 or KOH) in a precursor by a co-precipitation method and their activity for CO oxidation has been evaluated. This precipitant had a significant influence on the structural properties and the catalytic activity of the $CuMn_2$ catalysts for CO oxidation. The catalyst prepared by $KMnO_4$ as a precipitant exhibited the most excellent catalytic activity for CO oxidation due to their high oxygen mobility. Maintaining the same precursor, while changing the precipitant causes a change in the density of active sites which influence the CO oxidation. The calcination strategies of the precursor have a great influence on the activity of resulting catalysts. The calcination order with respect to the performance of catalyst for CO oxidation is as follows: reactive calcination> flowing air> stagnant air. The RC route is the most appropriate calcination strategy for the production of highly active $CuMn_{2RC1}$ catalyst for CO oxidation. The performance of catalysts was accordance with their characterization. Finally, we conclude that the choice of precipitant in the precursor has a significant effect in designing the most efficient CO oxidation catalyst.